AUT Journal of Mechanical Engineering

AUT J. Mech. Eng., 1(2) (2017) 179-190
DOI: 10.22060/mej.2017.12655.5389

Natural Frequency Analysis of Composite Skew Plates with Embedded Shape Memory Alloys in Thermal Environment

S. Kamarian, M. Shakeri*

Department of Mechanical Engineering, Amirkabir University of Technology, Tehran, Iran

ABSTRACT: In this study, free vibration analysis of laminated composite skew plates with embedded shape memory alloys under thermal loads is presented. The plates are assumed to be made of NiTi/Graphite/Epoxy with temperature-dependent properties. The thermo-mechanical behavior of shape memory alloy wires is predicted by employing one-dimensional Brinson's model. The governing equations are derived based on first-order shear deformation theory and solved using generalized differential quadrature technique as an efficient and accurate numerical tool. Some examples are provided to show the accuracy and efficiency of the applied numerical method by comparing the present results with those available in the literature. A parametric study is carried out to demonstrate the influence of skew angle, pre-strain and volume fraction of shape memory alloys, temperature, and stacking sequence of layers on the natural frequencies of the structure. Results represent that shape memory alloys can change the vibrational characteristics of shape memory alloy hybrid composite skew plates by a considerable amount. The numerical results also reveal that the effect of shape memory alloy wires on natural frequencies of composite plates with simply supported boundaries is higher than those with clamped boundaries.

Review History:

Received: 12 March 2017
Revised: 23 July 2017
Accepted: 24 July 2017
Available Online: 17 October 2017

Keywords:

Shape memory alloys
Hybrid composites
Skew plates
Natural frequency

1- Introduction

Composite plates are one of the most important structures in engineering applications. These structures are often used in thermal environments where they can generate thermal stresses and affect the vibrational characteristics of structure [1-5]. Although skew plates play an important role in engineering structures, only few research works have been devoted to analyzing the free vibration of laminated skew plates under thermal loads. Among those available, vibration behavior of thermally stressed laminated composite skew plates was discussed by Singha et al. [6]. They studied the first three natural frequencies of structure in both pre and post-buckled states and investigated the effects of some parameters like fiber orientation, skew angle, and boundary condition on the vibrations of the plate. Using various flexural theories, the vibration characteristics of thermally induced skew sandwich plates were examined by Heuer [7]. Recently, Singh and Chakrabarti [8] have used an efficient C^0 FE model developed based on refined higher order zigzag theory to investigate static, vibration, and thermal buckling of laminated composite skew plates. They showed that this model is able to satisfy the inter-laminar shear stress continuity at the interfaces and zero transverse shear stress conditions at top and bottom of the structure. A comparison was made between their results and the available data in the literature that showed the efficiency of the applied model for the analysis of skew plates.

A way of solving the problem related to induced thermal stresses because of the thermal environment which can have destructive effects on the stiffness of laminated composite structures is embedding Shape Memory Alloy (SMA) wires in the layers. It has been shown that SMAs are able to compensate the compressive thermal stresses by a considerable amount because of their extraordinary characteristics, namely Shape Memory Effect (SME) which can recover predetermined large strains when heated and Pseudo-Elasticity (PE) whereby SMAs show the pseudo-elasticity behavior and can recover large strains during mechanical loading-unloading patterns at high temperatures [9]. To this end, many experimental and numerical research works have been dedicated to highlight the influence of embedded SMA fibers on the natural frequency response of Shape Memory Alloys Hybrid Composite (SMAHC) structures. The vibration characteristics of laminated composites with embedded unidirectional and woven SMA was investigated experimentally by Zhang et al. [10]. For unidirectional case, the effect of both SMA arrangement and temperature on the natural frequency of structure was observed, and for the woven case, the influence of temperature and SMA volume fraction on the stiffness of plate was examined using vibration tests. The experimental results were compared with the analytical solution. The comparison showed a reasonable agreement between the numerical results and experimental responses. Yongsheng and Shuangshuang [11] studied free and forced flexural vibration of large deformation SMAHC plate using Brinson model. The boundary conditions were assumed to be simply supported and the vibrational response of structure was obtained employing Galerkin method. A parametric study was carried out to show the role of some parameters such as SMA volume fraction, temperature and aspect ratio on the dynamical behavior of the structure. The radial vibrations of SMAHC cylindrical shells under a harmonic internal pressure were analyzed using differential quadrature method and Newmark approach by Forouzesh and Jafari. [12]. The boundary conditions were taken to be simply supported, and the governing equations were derived based on Donnell-type classical shell theory and using Hamilton's

Corresponding author, E–mail: shakeri@aut.ac.ir

principle. Boyd–Lagoudas model was also implemented to predict the thermo-mechanical behavior of SMA fibers. Parhi and Singh [13] presented a nonlinear free vibration analysis of SMAHC spherical and cylindrical composite shell panels. The governing equations were derived based on the higher-order shear deformation plate theory using nonlinear von-Karman strain displacement relations and were solved by applying nine-nodded isoperimetric element. The influence of pre-strain of SMAs, volume fraction of SMAs, temperature, and curvature on the linear and non-linear frequency of structure were discussed in detail. A nonlinear dynamic analysis of a sandwich plate with the flexible core and SMAHC face sheets was provided by Dehkordi et al. [14] using the mixed Layer-Wise (LW)/ Equivalent Single Layer (ESL) models. In order to simulate the non-linear thermo-mechanical behavior of SMA fibers, Brinson model was applied. The effective parameters on the dynamic behavior of structure such as volume fraction, location of SMAs, the thickness of face sheets, plate aspect ratio, and boundary conditions were comprehensively studied. The nonlinear free vibration of thermally buckled SMAHC sandwich plate was examined by Samadpour et al. [15] using Brinson model. The nonlinear equations of motion were derived based on First-order Shear Deformation Theory (FSDT) and von Karman geometric nonlinearity through Hamilton principle, and the dynamic behavior of sandwich plates was investigated via Galerkin weighted residual method. The obtained results of this study showed that SMA fibers can significantly affect the natural frequency and post-buckling deflection of sandwich plates.

It can be found from the literature survey that, to the best of the authors' knowledge, there is no published work on the vibrational behavior of thermally induced laminated composite skew plates with the embedded SMA wires. Therefore, the present work aims to analyze natural frequency of SMAHC skew plates in thermal environment. A parametric study is presented to highlight the role of some parameters like pre-strain and volume fraction of SMAs, different boundary conditions, temperature, and thickness of plate on free vibration of laminated composite skew plates. The governing equations are derived based on FSDT via Hamilton principle, and the natural frequency parameters of the structure are obtained using Generalized Differential Quadrature (GDQ) approach. Some numerical examples are also provided to show the accuracy of the applied numerical method.

2- Problem Formulation

2- 1- Shape memory alloys

SMAs have a phase with high-temperature called austenite (A) and a low-temperature one, called martensite (M) which can be existed in two forms, twinned and detwinned martensite (Fig. 1). The reversible transformation from austenite to martensite and vice versa is the main reason for the incomparable behavior of SMAs. Brinson [9] introduced an acceptable model to predict SMA behavior which was matched with the experimental results. According to this model, the volume fraction of martensite phase is decomposed into two components as follows

$$\xi = \xi_s + \xi_T \tag{1}$$

where, ξ_T and ξ_s denote the volume fractions of martensite produced by temperature and stress, respectively. The modulus of elasticity, and generated stress can be obtained as

$$E(\xi) = E_A + \xi(E_A - E_M) \tag{2}$$

$$\sigma = E_s(\xi)(\varepsilon - \varepsilon_L \xi_s) + \alpha \Delta T \tag{3}$$

According to Ref. [9], martensite fraction during heating stage when $T > A_s$ and $C_A(T-A_f) < \sigma < C_A(T-A_s)$ can be calculated in the form of

$$\xi = \frac{\xi_0}{2}\left\{\cos\left[\frac{\pi}{A_f - A_s}\left(T - A_s - \frac{\sigma}{C_A}\right)\right] + 1\right\}$$
$$\xi_s = \xi_{s0}\frac{\xi}{\xi_0} \quad , \quad \xi_T = \xi_{T0}\frac{\xi}{\xi_0} \tag{4}$$

where subscript '0' indicates the initial state of a parameter. Also, A_f and A_s denote austenite start and austenite finish temperatures, respectively, and C_A represents the slope of the curve shown in Fig. 1 presumed to be constant. The details of Brinson model are comprehensively explained in Ref. [9]. The properties of SMA/fiber/epoxy composites can be obtained using the following relations

$$E_1 = E_S(\xi)V_S + E_{1m}(1 - V_S);$$
$$E_2 = E_{2m}\left[(1-\sqrt{V_S}) + \frac{\sqrt{V_S}}{1-\sqrt{V_S}(1-\frac{E_{2m}}{E_S(\xi)})}\right]$$
$$G_{12} = G_{13} = G_{12m}\left[(1-\sqrt{V_S}) + \frac{\sqrt{V_S}}{1-\sqrt{V_S}(1-\frac{G_{12m}}{G_S(\xi)})}\right];$$
$$G_S(\xi) = \frac{E_S(\xi)}{2(1+\nu_{12S})} \tag{5}$$
$$\alpha_1 = \frac{V_S\alpha_S E_S(\xi) + (1-V_S)\alpha_{1m}E_{1m}}{E_1};$$
$$\alpha_2 = \frac{E_{2m}}{E_2}\left[\alpha_{2m}(1-\sqrt{V_S}) + \frac{\alpha_{2m}\sqrt{V_S} - V_S(\alpha_{2m}-\alpha_S)}{1-\sqrt{V_S}(1-\frac{E_{2m}}{E_S(\xi)})}\right]$$
$$\nu_{12} = \nu_{12S}V_S + \nu_{12m}(1-V_S);$$
$$\rho = \rho_S V_S + \rho_m(1-V_S)$$

where the subscripts 'm' and 's' mean the composite matrix and SMA fiber, respectively. Moreover, parameters E, G, ν, α, ρ and V_s denote Young modulus, shear modulus, Poisson ratio, thermal expansion coefficient, material density and volume fraction of SMA fibers, respectively.

2- 2- Governing equations

Consider a rectangular composite plate with the lengths of a and b, and the thickness of h, as shown in Fig. 2(a). Based on FSDT, the displacement components are obtained as

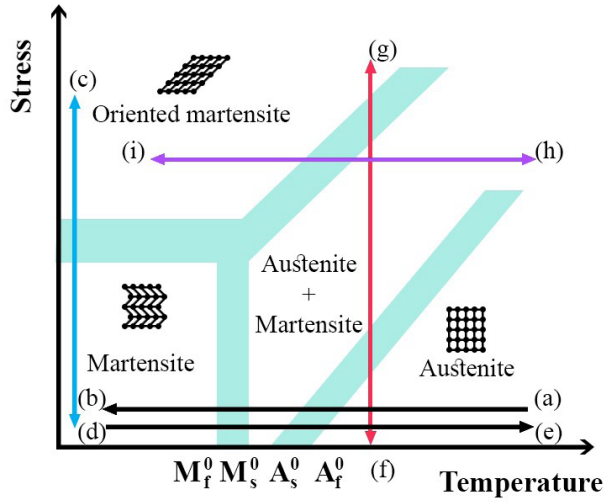

Fig. 1. Schematic phase diagram for SMAs

$$\begin{aligned} u(x,y,z,t) &= u_0(x,y,t) + z\,\phi_x(x,y,t) \\ v(x,y,z,t) &= v_0(x,y,t) + z\,\phi_y(x,y,t) \\ w(x,y,z,t) &= w_0(x,y,t) \end{aligned} \tag{6}$$

where u_0 and v_0 are the displacements of the middle surface in the x and y directions, w_0 is the transverse deflection, and φ_x and φ_y are the rotations of the middle surface of the plate about x and y axes, respectively. The strain-displacement relations are defined as

$$\begin{Bmatrix} \varepsilon_{xx} \\ \varepsilon_{yy} \\ \gamma_{yz} \\ \gamma_{xz} \\ \gamma_{xy} \end{Bmatrix} = \begin{Bmatrix} \dfrac{\partial u_0}{\partial x} \\ \dfrac{\partial v_0}{\partial y} \\ \dfrac{\partial w_0}{\partial y} + \phi_y \\ \dfrac{\partial w_0}{\partial x} + \phi_x \\ \dfrac{\partial u_0}{\partial y} + \dfrac{\partial v_0}{\partial x} \end{Bmatrix} + z \begin{Bmatrix} \dfrac{\partial \phi_x}{\partial x} \\ \dfrac{\partial \phi_y}{\partial y} \\ 0 \\ 0 \\ \dfrac{\partial \phi_x}{\partial y} + \dfrac{\partial \phi_y}{\partial x} \end{Bmatrix} \tag{7}$$

The constitutive law for SMAHC plates under thermal loads are as follows

$$\begin{bmatrix} \sigma_{xx} \\ \sigma_{yy} \\ \tau_{yz} \\ \tau_{xz} \\ \tau_{xy} \end{bmatrix} = \begin{bmatrix} \bar{Q}_{11} & \bar{Q}_{12} & 0 & 0 & \bar{Q}_{16} \\ \bar{Q}_{12} & \bar{Q}_{22} & 0 & 0 & \bar{Q}_{26} \\ 0 & 0 & \bar{Q}_{44} & 0 & 0 \\ 0 & 0 & 0 & \bar{Q}_{55} & 0 \\ \bar{Q}_{16} & \bar{Q}_{26} & 0 & 0 & \bar{Q}_{66} \end{bmatrix} \times \left(\begin{bmatrix} \varepsilon_{xx} \\ \varepsilon_{yy} \\ \varepsilon_{yz} \\ \varepsilon_{xz} \\ \varepsilon_{xy} \end{bmatrix} - \Delta T \begin{bmatrix} \alpha_{xx} \\ \alpha_{yy} \\ 0 \\ 0 \\ 2\alpha_{xy} \end{bmatrix} \right) + V_s \begin{bmatrix} \sigma_x^r \\ \sigma_y^r \\ 0 \\ 0 \\ \sigma_{xy}^r \end{bmatrix} \tag{8}$$

where $\Delta T = T - T_0$, T_0 is the reference temperature, T denotes the temperature of the structure, $\bar{Q}_{ij}$ represents the plane stress-reduced stiffness, and α_{ij} are thermal expansion coefficients which all can be found in Ref. [15]. The stress resultants can be calculated as

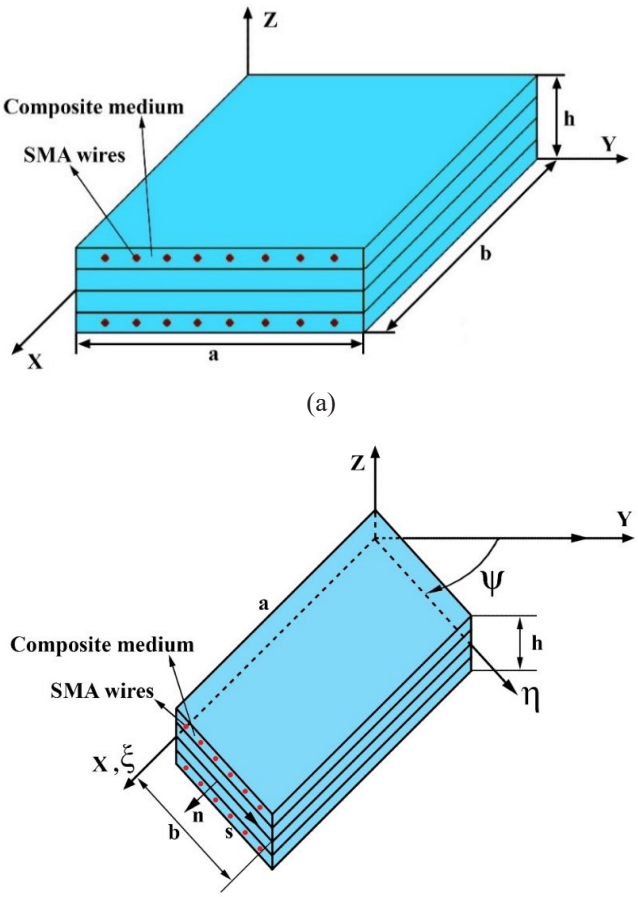

Fig. 2. Schematic of the rectangular and skew composite plates with embedded SMA in bottom and top layers

$$\begin{Bmatrix} N_x \\ N_y \\ N_{xy} \\ M_x \\ M_y \\ M_{xy} \end{Bmatrix} = \int_{-h/2}^{h/2} \begin{bmatrix} \sigma_{xx} \\ \sigma_{yy} \\ \tau_{yz} \\ \sigma_{xx}\, z \\ \sigma_{yy}\, z \\ \tau_{xy}\, z \end{bmatrix} dz = \begin{bmatrix} A_{11} & A_{12} & A_{16} & B_{11} & B_{12} & B_{16} \\ A_{12} & A_{22} & A_{26} & B_{12} & B_{22} & B_{26} \\ A_{16} & A_{26} & A_{66} & B_{16} & B_{26} & B_{66} \\ B_{11} & B_{12} & B_{16} & D_{11} & D_{12} & D_{16} \\ B_{12} & B_{22} & B_{26} & D_{12} & D_{22} & D_{26} \\ B_{16} & B_{26} & B_{66} & D_{16} & D_{26} & D_{66} \end{bmatrix} \begin{Bmatrix} \dfrac{\partial u_0}{\partial x} \\ \dfrac{\partial v_0}{\partial y} \\ \dfrac{\partial u_0}{\partial y} + \dfrac{\partial v_0}{\partial x} \\ \dfrac{\partial \phi_x}{\partial x} \\ \dfrac{\partial \phi_y}{\partial y} \\ \dfrac{\partial \phi_x}{\partial y} + \dfrac{\partial \phi_y}{\partial x} \end{Bmatrix} \tag{9}$$

$$-\begin{Bmatrix} N_x^T \\ N_y^T \\ N_{xy}^T \\ M_x^T \\ M_y^T \\ M_{xy}^T \end{Bmatrix} + \begin{Bmatrix} N_x^r \\ N_y^r \\ N_{xy}^r \\ M_x^r \\ M_y^r \\ M_{xy}^r \end{Bmatrix}$$

$$\begin{Bmatrix} Q_y \\ Q_x \end{Bmatrix} = k_s \int_{-h/2}^{h/2} \begin{bmatrix} \tau_{yz} \\ \tau_{xz} \end{bmatrix} dz = k_s \begin{bmatrix} A_{44} & A_{45} \\ A_{45} & A_{55} \end{bmatrix} \begin{Bmatrix} \frac{\partial w_0}{\partial y} + \phi_y \\ \frac{\partial w_0}{\partial x} + \phi_x \end{Bmatrix}$$

where k_s is the shear correction factor, N^T and M^T represent the thermal force and thermal moment resultants, and; furthermore, N^r and M^r indicate the induced force and bending moment resultants by SMA wires defined as

$$\begin{Bmatrix} N_x, M_x \\ N_y, M_y \\ N_{xy}, M_{xy} \end{Bmatrix}^T = \sum_{k=1}^{N} \int_{h_{k-1}}^{h_k} \begin{bmatrix} \overline{Q}_{11} & \overline{Q}_{12} & \overline{Q}_{16} \\ \overline{Q}_{12} & \overline{Q}_{22} & \overline{Q}_{26} \\ \overline{Q}_{16} & \overline{Q}_{26} & \overline{Q}_{66} \end{bmatrix}^{(k)} \begin{bmatrix} \alpha_x(T) \\ \alpha_y(T) \\ \alpha_{xy}(T) \end{bmatrix}^{(k)} \Delta T\,(1,z)\,dz \quad (10a)$$

$$\begin{Bmatrix} N_x, M_x \\ N_y, M_y \\ N_{xy}, M_{xy} \end{Bmatrix}^r = \sum_{k=1}^{N} \int_{h_{k-1}}^{h_k} V_s \sigma^r \begin{Bmatrix} \cos^2(\theta^k) \\ \sin^2(\theta^k) \\ \sin(\theta^k)\cos(\theta^k) \end{Bmatrix} (1,z)\,dz \quad (10b)$$

Using Hamilton's principle, the out-of-plane free vibration equations of rectangular composite plates can be yielded as

$$\frac{\partial M_{xx}}{\partial x} + \frac{\partial M_{xy}}{\partial y} - Q_x = I_2 \frac{\partial^2 \phi_x}{\partial t^2} \quad (11a)$$

$$\frac{\partial M_{xy}}{\partial x} + \frac{\partial M_{yy}}{\partial y} - Q_y = I_2 \frac{\partial^2 \phi_y}{\partial t^2} \quad (11b)$$

$$\frac{\partial Q_x}{\partial x} + \frac{\partial Q_y}{\partial y} + \left(N_{xx} \frac{\partial^2 w_0}{\partial x^2} + 2N_{xy} \frac{\partial^2 w_0}{\partial x y} + N_{yy} \frac{\partial^2 w_0}{\partial y^2} \right) = I_0 \frac{\partial^2 w_0}{\partial t^2} \quad (11c)$$

In the present work, simply supported and clamped boundary conditions are considered. From pre-buckling analysis, the non-linear terms, involving N_x, N_y and N_{xy} in Eq. (11c) are ignored [16]. Thus, by inserting Eq. (9) into Eq. (11), the out-of-plane free vibration equations of rectangular SMAHC plates in thermal environments can be obtained as

$$D_{11}\left(\frac{\partial^2 \varphi_x}{\partial x^2}\right) + D_{12}\left(\frac{\partial^2 \varphi_y}{\partial x \partial y}\right) + D_{66}\left(\frac{\partial^2 \varphi_x}{\partial y^2} + \frac{\partial^2 \varphi_y}{\partial x \partial y}\right) - k_s A_{55}\left(\varphi_x + \frac{\partial w}{\partial x}\right) - k_s A_{45}\left(\varphi_y + \frac{\partial w}{\partial y}\right) + 2D_{16}\frac{\partial^2 \varphi_x}{\partial x \partial y} + D_{16}\frac{\partial^2 \varphi_y}{\partial x^2} + D_{26}\frac{\partial^2 \varphi_y}{\partial y^2} = I_2 \frac{\partial^2 \varphi_x}{\partial t^2} \quad (12a)$$

$$D_{66}\left(\frac{\partial^2 \varphi_y}{\partial x^2} + \frac{\partial^2 \varphi_x}{\partial x \partial y}\right) + D_{12}\left(\frac{\partial^2 \varphi_x}{\partial x \partial y}\right) + D_{22}\left(\frac{\partial^2 \varphi_y}{\partial y^2}\right) - k_s A_{44}\left(\varphi_y + \frac{\partial w}{\partial y}\right) - k_s A_{45}\left(\varphi_x + \frac{\partial w}{\partial x}\right) + D_{16}\frac{\partial^2 \varphi_x}{\partial x^2} + D_{26}\frac{\partial^2 \varphi_x}{\partial y^2} + 2D_{26}\frac{\partial^2 \varphi_y}{\partial x \partial y} = I_2 \frac{\partial^2 \varphi_y}{\partial t^2} \quad (12b)$$

$$k_s A_{55}\left(\frac{\partial \varphi_x}{\partial x} + \frac{\partial^2 w}{\partial x^2}\right) + k_s A_{44}\left(\frac{\partial \varphi_y}{\partial y} + \frac{\partial^2 w}{\partial y^2}\right) + k_s A_{45}\left(\frac{\partial \varphi_x}{\partial y} + \frac{\partial \varphi_y}{\partial x} + 2\frac{\partial^2 w}{\partial x \partial y}\right) + (N_x^r - N_x^T)\frac{\partial^2 w}{\partial x^2} + 2(N_{xy}^r - N_{xy}^T)\frac{\partial^2 w}{\partial x \partial y} + (N_y^r - N_y^T)\frac{\partial^2 w}{\partial y^2} = I_0 \frac{\partial^2 w}{\partial t^2} \quad (12c)$$

Eqs. (12a-12c) are governed for SMAHC rectangular composite plates, however the aim of this paper is to analyze thermal vibrations of SMAHC skew plates. The easiest way to derive the free vibration equations of skew plates is to transform the *x*-*y* equations into ζ-η domain (Fig. 2(b)). To this end, the following linear transformation rules are employed to Eqs. (12a-12c).

$$x = \xi + (\sin\psi)\eta \ , \ y = (\cos\psi)\eta \quad (13)$$

Thus, the governing equations for the vibration of composite skew plates can be derived as:

$$\begin{aligned} &\left(D_{11} - 2D_{16}\tan\psi + D_{66}\tan^2\psi\right)\frac{\partial^2 \varphi_x}{\partial \zeta^2} \\ &+2\sec\psi\left(D_{16} - \tan\psi D_{66}\right)\frac{\partial^2 \varphi_x}{\partial \zeta \partial \eta} \\ &+\left(\sec^2\psi D_{66}\right)\frac{\partial^2 \varphi_x}{\partial \eta^2} - k_s A_{55}\varphi_x \\ &+[D_{16} - \tan\psi(D_{12} + D_{66}) + D_{26}\tan^2\psi]\frac{\partial^2 \varphi_y}{\partial \zeta^2} \\ &+\sec\psi\left(D_{12} + D_{66} - 2\tan\psi D_{26}\right)\frac{\partial^2 \varphi_y}{\partial \zeta \partial \eta} \\ &+\left(\sec^2\psi D_{26}\right)\frac{\partial^2 \varphi_y}{\partial \eta^2} - k_s A_{45}\varphi_y \\ &+\left(\tan\psi k_s A_{45} - k_s A_{55}\right)\frac{\partial w}{\partial \zeta} \\ &+\left(-\sec\psi k_s A_{45}\right)\frac{\partial w}{\partial \eta} = I_2 \frac{\partial^2 \varphi_x}{\partial t^2} \end{aligned} \quad (14a)$$

$$\begin{aligned} &[D_{16} - (D_{12} + D_{66})\tan\psi \\ &+D_{26}\tan^2\psi]\frac{\partial^2 \varphi_x}{\partial \zeta^2} \end{aligned} \quad (14b)$$

$$+\sec\psi\left(D_{12}+D_{66}-2D_{26}\tan\psi\right)\frac{\partial^2\varphi_x}{\partial\zeta\partial\eta}$$
$$+D_{26}\sec^2\psi\frac{\partial^2\varphi_x}{\partial\eta^2}$$
$$+(D_{66}-2D_{26}\tan\psi+D_{22}\tan^2\psi)\frac{\partial^2\varphi_y}{\partial\zeta^2}$$
$$+2\sec\psi\left(D_{26}-D_{22}\tan\psi\right)\frac{\partial^2\varphi_y}{\partial\zeta\partial\eta}$$
$$+D_{22}\sec^2\psi\frac{\partial^2\varphi_y}{\partial\eta^2}$$
$$+\left(k_sA_{44}\tan\psi-A_{45}\right)\frac{\partial w}{\partial\zeta}$$
$$-k_sA_{44}\sec\psi\frac{\partial w}{\partial\eta}-k_sA_{45}\varphi_x$$
$$-k_sA_{44}\varphi_y=I_2\frac{\partial^2\varphi_y}{\partial t^2}$$

$$k_s\left(A_{55}-A_{45}\tan\psi\right)\frac{\partial\varphi_x}{\partial\zeta}+A_{45}\sec\psi\frac{\partial\varphi_x}{\partial\eta}$$
$$+k_s\left(A_{45}-A_{44}\tan\psi\right)\frac{\partial\varphi_y}{\partial\zeta}+k_sA_{44}\sec\psi\frac{\partial\varphi_y}{\partial\eta}$$
$$+k_s\left(A_{55}-2A_{45}\tan\psi+A_{44}\tan^2\psi\right)\frac{\partial^2w}{\partial\zeta^2}$$
$$+2k_s\left(A_{45}-A_{44}\tan\psi\right)\sec\psi\frac{\partial^2w}{\partial\zeta\partial\eta}$$
$$+k_sA_{44}\sec^2\psi\frac{\partial^2w}{\partial\eta^2}$$
$$+[(N_{xx}^T-N_{xx}^r)-2(N_{xy}^T-N_{xy}^r)\tan\psi$$
$$+(N_{yy}^T-N_{yy}^r)\tan^2\psi]\frac{\partial^2w}{\partial\zeta^2}$$
$$+2\sec\psi[(N_{xy}^T-N_{xy}^r)$$
$$-(N_{yy}^T-N_{yy}^r)\tan\psi]\frac{\partial^2w}{\partial\zeta\partial\eta}$$
$$+(N_{yy}^T-N_{yy}^r)\sec^2\psi\frac{\partial^2w}{\partial\eta^2}=I_0\frac{\partial^2w}{\partial t^2}\qquad(14c)$$

As mentioned before, in the present study, SMAHC skew plates with simply supported or clamped boundary conditions are considered. The boundary conditions of plates are specified by the letter symbols. For example, SCSC represents that the plate is simply supported at x=0 , a and is clamped at y=0 , b. The conditions for the clamped (C) and simply supported (S) edges become

$$\textit{Clamped}:\quad W=0\ ;\ \varphi^s=-n_y\varphi^x+n_x\varphi^y=0\ ;\ \varphi^n=n_x\varphi^x+n_y\varphi^y=0\qquad(15a)$$

$$\textit{Simply Supported}:\quad W=0\ ;\ \varphi^s=-n_y\varphi^x+n_x\varphi^y=0\ ;\quad M_{nn}=M_{xx}n_x^2+M_{yy}n_y^2+2M_{xy}n_xn_y=0\qquad(15b)$$

where n_x and n_y are the x- and y-components of the unit normal vector to an arbitrary edge of the plate, respectively.

2- 3- GDQ method

In the present work, GDQ method is used to obtain the natural frequencies of SMAHC skew plates. Assume a continuous function $f(\zeta,\eta)$ having its field on a $0\le\zeta\le a$, $0\le\eta\le b$. Based on this approach, the rth order of the function with respect to ζ, at point (ζ_i,η_i) can be approximated as [17, 18]:

$$\left.\frac{f^{\,r}(\zeta,\eta)}{\partial\zeta^r}\right|_{(\zeta,\eta)=(\zeta_i,\eta_j)}=\sum_{m=1}^{N_\zeta}A_{im}^{\zeta(r)}f(\zeta_m,\eta_j)=\sum_{m=1}^{N_\zeta}c_{im}^{\zeta(r)}f_{mj}\ ,\qquad(16)$$
$$i=1,2,...,N_\zeta\ ,\ r=1,2,...,N_\zeta-1$$

From Eq. (16), one can see that the important components of DQ method are weighting coefficients and the choice of sampling points. The weighting coefficients for the first-order derivatives in the ζ- direction are determined as [17, 18]

$$c_{ij}^{\zeta(1)}=A_{ij}^{\zeta}=\frac{1}{a}\begin{cases}\dfrac{M(\zeta_i)}{(\zeta_i-\zeta_j)M(\zeta_j)} & for\quad i\ne j\\ -\sum\limits_{\substack{j=1\\ i\ne j}}^{N_\zeta}A_{ij}^{\zeta} & for\quad i=j\end{cases}\qquad i,j=1,2,...,N_\zeta\qquad(17)$$

where $M(\zeta_i)=\prod_{j=1,i\ne j}^{N_\zeta}(\zeta_i-\zeta_j)$

The weighting coefficients for second-order derivatives in the ζ- direction are also determined as

$$[c_{ij}^{\zeta(2)}]=[B_{ij}^{\zeta}]=[A_{ij}^{\zeta}][A_{ij}^{\zeta}]=[A_{ij}^{\zeta}]^2\qquad(18)$$

Similarly, the weighting coefficients for ζ- direction can be obtained. Here, Chebyshev–Gauss–Lobatto quadrature points are used, that is [17]

$$\zeta_i=\frac{a}{2}\left[1-\cos\left[\frac{(i-1)\pi}{(N_\zeta-1)}\right]\right],$$
$$\eta_j=\frac{b}{2}\left[1-\cos\left[\frac{(j-1)\pi}{(N_\eta-1)}\right]\right];\qquad(19)$$
$$i=1,2,...,N_\zeta\ ,\ j=1,2,...,N_\eta$$

Applying GDQ method on the free vibration equations, the following discretized equations are obtained.

$$\left(D_{11}-2D_{16}\tan\psi+D_{66}\tan^2\psi\right)\sum_{m=1}^{N_\zeta}B_{im}^{\zeta}\varphi_{mj}^x$$
$$+2\left(D_{16}-D_{66}\tan\psi\right)\sec\psi\sum_{m=1}^{N_\zeta}\sum_{n=1}^{N_\eta}A_{im}^{\zeta}A_{jn}^{\eta}\varphi_{mn}^x$$
$$+D_{66}\sec^2\psi\sum_{n=1}^{N_\eta}B_{jn}^{\eta}\varphi_{in}^x-k_sA_{55}\varphi_{ij}^x$$
$$+[D_{16}-(D_{12}+D_{66})\tan\psi+D_{26}\tan^2\psi]\sum_{m=1}^{N_\zeta}B_{im}^{\zeta}\varphi_{mj}^y\qquad(20a)$$
$$+\left(D_{12}+D_{66}-2D_{26}\tan\psi\right)\sec\psi\sum_{m=1}^{N_\zeta}\sum_{n=1}^{N_\eta}A_{im}^{\zeta}A_{jn}^{\eta}\varphi_{mn}^y$$
$$+D_{26}\sec^2\psi\sum_{n=1}^{N_\eta}B_{jn}^{\eta}\varphi_{in}^y-k_sA_{45}\varphi_{ij}^y+$$

$$
\begin{aligned}
&k_s\left(A_{45}\tan\psi - A_{55}\right)\sum_{m=1}^{N_\zeta} A_{im}^{\zeta} w_{mj} - k_s A_{45}\sec\psi\sum_{n=1}^{N_\eta} A_{jn}^{\eta} w_{in} \\
&= I_2\frac{\partial^2\varphi_{ij}^x}{\partial t^2}
\end{aligned}
$$

$$
\begin{aligned}
&[D_{16} - (D_{12}+D_{66})\tan\psi + D_{26}\tan^2\psi]\sum_{m=1}^{N_\zeta} B_{im}^{\zeta}\varphi_{mj}^x \\
&+\left(D_{12}+D_{66}-2D_{26}\tan\psi\right)\sec\psi\sum_{m=1}^{N_\zeta}\sum_{n=1}^{N_\eta} A_{im}^{\zeta}A_{jn}^{\eta}\varphi_{mn}^x \\
&+D_{26}\sec^2\psi\sum_{n=1}^{N_\eta} B_{jn}^{\eta}\varphi_{in}^x - k_s A_{45}\varphi_{ij}^x \\
&+(D_{66}-2D_{26}\tan\psi + D_{22}\tan^2\psi)\sum_{m=1}^{N_\zeta} B_{im}^{\zeta}\varphi_{mj}^y \\
&+2\left(D_{26}-D_{22}\tan\psi\right)\sec\psi\sum_{m=1}^{N_\zeta}\sum_{n=1}^{N_\eta} A_{im}^{\zeta}A_{jn}^{\eta}\varphi_{mn}^y \\
&+D_{22}\sec^2\psi\sum_{n=1}^{N_\eta} B_{jn}^{\eta}\varphi_{in}^y\frac{\partial^2\varphi_y}{\partial\eta^2} - k_s A_{44}\varphi_{ij}^y \\
&+\left(k_s A_{44}\tan\psi - A_{45}\right)\sum_{m=1}^{N_\zeta} A_{im}^{\zeta} w_{mj} - k_s A_{44}\sec\psi\sum_{n=1}^{N_\eta} A_{jn}^{\eta} w_{in} \\
&= I_2\frac{\partial^2\varphi_y}{\partial t^2}
\end{aligned}
\tag{20b}
$$

$$
\begin{aligned}
&k_s\left(A_{55} - A_{45}\tan\psi\right)\sum_{m=1}^{N_\zeta} A_{im}^{\zeta}\varphi_{mj}^x \\
&+A_{45}\sec\psi\sum_{n=1}^{N_\eta} A_{jn}^{\eta}\varphi_{in}^x \\
&+k_s\left(A_{45} - A_{44}\tan\psi\right)\sum_{m=1}^{N_\zeta} A_{im}^{\zeta}\varphi_{mj}^y \\
&+k_s A_{44}\sec\psi\sum_{n=1}^{N_\eta} A_{jn}^{\eta}\varphi_{in}^y \\
&+k_s(A_{55} - 2A_{45}\tan\psi + A_{44}\tan^2\psi)\sum_{m=1}^{N_\zeta} B_{im}^{\zeta} w_{mj} \\
&+2k_s\left(A_{45} - A_{44}\tan\psi\right)\sec\psi\sum_{m=1}^{N_\zeta}\sum_{n=1}^{N_\eta} A_{im}^{\zeta}A_{jn}^{\eta} w_{mn} \\
&+k_s A_{44}\sec^2\psi\sum_{n=1}^{N\eta} B_{jn}^{\eta} w_{in} \\
&+[(N_{xx}^T - N_{xx}^r) - 2(N_{xy}^T - N_{xy}^r)\tan\psi \\
&+(N_{yy}^T - N_{yy}^r)\tan^2\psi]\sum_{m=1}^{N_\zeta} B_{im}^{\zeta} w_{mj} \\
&+2\sec\psi[(N_{xy}^T - N_{xy}^r) \\
&-(N_{yy}^T - N_{yy}^r)\tan\psi]\sum_{m=1}^{N_\zeta}\sum_{n=1}^{N_\eta} A_{im}^{\zeta}A_{jn}^{\eta} w_{mn} \\
&+(N_{yy}^T - N_{yy}^r)\sec^2\psi\sum_{m=1}^{N_\eta} B_{jn}^{\eta} w_{in} = I_0\frac{\partial^2 w}{\partial t^2}
\end{aligned}
\tag{20c}
$$

The GDQ approach is also applied to the boundary conditions of Eqs. (15a-15b)

Clamped :

$$
\begin{aligned}
&W_{ij} = 0\ ; \\
&\varphi_{ij}^s = -n_y\varphi_{ij}^x + n_x\varphi_{ij}^y = 0; \\
&\varphi_{ij}^n = n_x\varphi_{ij}^x + n_y\varphi_{ij}^y = 0
\end{aligned}
\tag{21a}
$$

Simply Supported :

$$
\begin{aligned}
&W_{ij} = 0\ ;\ \varphi_{ij}^s = -n_y\varphi_{ij}^x + n_x\varphi_{ij}^y = 0\ ; \\
&M_{nn})_{ij} = [n_x^2 D_{11} + 2n_x n_y D_{16} + n_y^2 D_{12} \\
&-(n_x^2 D_{16} + 2n_x n_y D_{66} + n_y^2 D_{26})\tan\psi]\sum_{m=1}^{N_\zeta} A_{im}^{\zeta}\varphi_{mj}^x + \\
&[n_x^2 D_{16} + 2n_x n_y D_{66} + n_y^2 D_{26} \\
&-(n_x^2 D_{12} + 2n_x n_y D_{26} + n_y^2 D_{22})\tan\psi]\sum_{n=1}^{N_\eta} A_{jn}^{\eta}\varphi_{in}^y = 0
\end{aligned}
\tag{21b}
$$

Thus, the matrix form of the discretized equations of motion and boundary conditions can be written as equations of motion:

$$[S_{db}]\{U_b\} + [S_{dd}]\{U_d\} + [M]\{\ddot{U}_d\} = \{0\} \tag{22a}$$

$$[S_{bb}]\{U_b\} + [S_{bd}]\{U_d\} = \{0\} \tag{22b}$$

where $\{U_d\}$ and $\{U_b\}$ are the domain and the boundary degrees of freedom, respectively. Also, $[S_{ij}]$ and $[M_{ij}]$ with $(i,j=b,d)$ denote the stiffness and mass matrices, respectively. Combining Eqs. (22a) and (22b) and also considering the harmonic nature of the motion, the following standard eigenvalue problem can be obtained.

$$([S] - \omega^2[M])\{\tilde{U}_d\} = \{0\} \tag{23}$$

where $[S]=[S_{dd}]-[S_{dd}][S_{bb}]^{-1}[S_{bd}]$; ω is the natural frequency of SMAHC skew plate, and $\{\tilde{U}_d\}$ is the amplitude of motion. As can be seen, the natural frequencies of the structure can be obtained from Eq. (23).

3- Results and Discussion

In this section, free vibration analysis of SMAHC skew plates is studied. To this end, first, a comparative study is provided to verify the present numerical solution. Then, the importance of some parameters such as stacking sequence of layers, volume fraction and pre-strain of SMA wires and geometrical parameters in the natural frequency response of SMAHC skew plate is highlighted. As shown in Fig. 2(b), in the present work, the SMA wires are supposed to be embedded in the outermost layers called SMA reinforced layers, and be aligned to the Graphite fibers. The skew plate is assumed to be made of NiTi/Graphite/Epoxy with temperature-dependent properties shown in Tables 1 and 2. The vibrational behavior of the structure is evaluated by defining a non-dimensional frequency parameter, $\Omega = \omega\left(\frac{a}{\pi}\right)^2\frac{1}{h}\sqrt{\frac{\rho_m}{E_{2m}}}$, in which ρ_m and E_{2m} are the density and transverse modulus of graphite/epoxy matrix, respectively.

Table 1. The material properties of graphite/epoxy [15]

Value	Unit
E_A=67	GPa
E_M=26.3	GPa
M_f=9	°C
M_s=18.4	°C
A_s=34.5	°C
A_f=49	°C
C_M=8	MP/ °C
C_A=13.8	MP/ °C
ε_L=0.067	-
v_s=0.33	-
α_s=10.26×10^{-6}	1/ °C
Θ=0.55	MP/ °C

Table 2. The material properties of graphite-epoxy

Properties		
$E_{1m}=E^0_{1m}(1+E^1_{1m}\Delta T)$;	E^0_{1m}=155;	E^1_{1m}=-3.53×10^{-4};
$E_{2m}=E^0_{2m}(1+E^1_{2m}\Delta T)$;	E^0_{2m}=8.07;	E^1_{2m}=-4.27×10^{-4};
$G_{12m}=G^0_{12m}(1+G^1_{12m}\Delta T)$;	G^0_{12m}=4.55;	G^1_{12m}=-6.06×10^{-4};
$\alpha_{1m}=\alpha^0_{1m}(1+\alpha^1_{1m}\Delta T)$;	α^0_{1m}=-0.07;	α^1_{1m}=-1.25×10^{-4};
$\alpha_{2m}=\alpha^0_{2m}(1+\alpha^1_{2m}\Delta T)$;	α^0_{2m}=30.1;	α^1_{2m}=0.41×10^{-4};
v_{12m}=0.22		

3- 1- Verification of numerical results

The accuracy of the applied numerical method is investigated by providing three examples. In the first example, the non-dimensional buckling temperatures of composite skew plates obtained from the present work are compared with other available data in the literature for different skew angles and boundary conditions. To this aim, the temperature of environment is increased until the frequency of structure reaches to zero. The material properties are assumed to be as follows:

$$\frac{E_1}{E_2}=15\ ,\ E_2=E_3\ ,\ \frac{G_{12}}{E_2}=\frac{G_{13}}{E_2}=0.5\ ,\ \frac{G_{23}}{E_2}=0.3356\ ,$$

$$\frac{\alpha_1}{\alpha_0}=0.015\ ,\ \frac{\alpha_2}{\alpha_0}=\frac{\alpha_3}{\alpha_0}=1\ ,\quad \alpha_0=1\times10^{-6}/^\circ C$$

It is observed from Table 3 that GDQ results are in a good agreement with those reported in Refs. [19, 20] and this numerical method is able to handle the analysis of composite skew plates in the pre-buckling domain. Further verification of GDQ results is studied by comparing the natural frequency of SMAHC rectangular plates with similar results obtained by an analytical solution discussed in Ref. [21], as depicted in Fig 3. The numbers in parentheses denote the vibrational modes of analytical solution. The analytical results of Fig. 3 state that for ΔT <236°C, the mode (1,1) yields a minimum natural frequency of the structure, while for ΔT > 236°C, the fundamental natural frequency of plate occurs at mode (1, 2). However, it was also observed that fundamental natural frequencies of GDQ approach fit analytical results very well and it can obtain the fundamental natural frequencies of

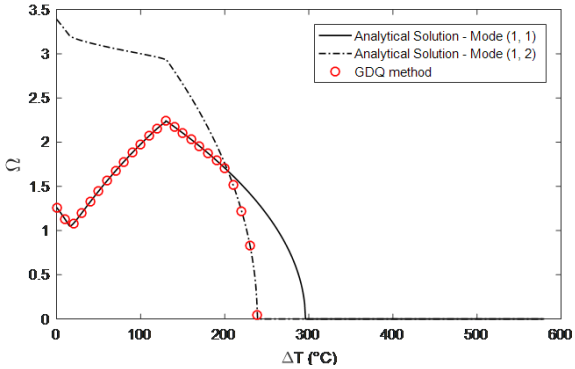

Fig. 3. Comparison of analytical solution with GDQ results for natural frequencies of SMAHC rectangular plates under thermal environment in pre-buckling region

Table 3. Comparison of critical buckling temperature parameters ($\lambda_T=\alpha_0 T_{cr}$) of [0° / 90°]$_s$ skew plates (a/b=1 , h/b=0.1 , α_0=10^{-6} 1/°C)

Boundary Conditions	ψ	Present	[19]	[20]
SSSS	0	0.0778	0.0770	-
	15	0.0799	0.0784	0.0794
	30	0.0888	0.0849	0.0860
	45	0.1129	0.1031	0.1041
SCSC	0	0.1091	0.1069	-
	15	0.1132	0.1108	0.1134
	30	0.1277	0.1243	0.1286
	45	0.1588	0.1533	0.1619
CCCC	0	0.1691	0.1655	-
	15	0.1712	0.1674	0.1712
	30	0.1799	0.1753	0.1799
	45	0.2041	0.1982	0.2044

Table 4. Comparison of the critical temperature of SMAHC rectangular plates (a/b=1 , h/b=1/50)

V_s	[90°,0°,90°,0°]$_s$		[0°,0°,90°,0°]$_s$	
	present	[22]	present	[22]
Without SMA	210	204 (1,1)	208	205 (1,1)
5%	237	231(1,1)	237	233(1,1)
10%	263	259(1,1)	250	252(1,2)
15%	291	286(1,1)	262	261(1,2)
20%	318	313(1,1)	272	272(1,2)
30%	372	367(1,1)	292	294(1,2)

*The numbers in the parentheses indicate the buckling modes from analytical solution

SMAHC plates with a high accuracy. The third numerical example is presented to show the validity of applied Brinson model. In this example, critical buckling temperatures of rectangular SMAHC plates are compared with those obtained by Asadi et al. [22]. Table 4 reveals that. To this aim, the temperature is increased until the frequency of structures reaches to zero. Table 4 reveals that GDQ can yield the buckling temperature of SMAHC plate with a negligible error.

3- 2- Temperature dependency of materials

The influence of temperature dependency of material properties on vibrational behavior of SMAHC skew plates is illustrated in Fig. 4. In this figure, TD represents the temperature dependent material properties and TID means the material properties do not change with variations of temperature(E^1_{1m}, E^1_{2m}, G^1_{12m}, α^1_{1m}, α^1_{2m}=0). This figure illustrates the variations of fundamental frequency parameters of an eight-layer $[30^o/-45^o/45^o/90^o]_s$ SMAHC skew plates with simply supported boundaries against temperature. From the diagrams of Fig. 4, two conclusions can be inferred; 1: materials with TD properties lead to a more natural frequency, compared to the TID ones, and 2: the effect of temperature dependency on the vibrations of SMAHC plates becomes more considerable by increasing SMA volume fraction. In next sections, only materials with TD properties are considered for the study.

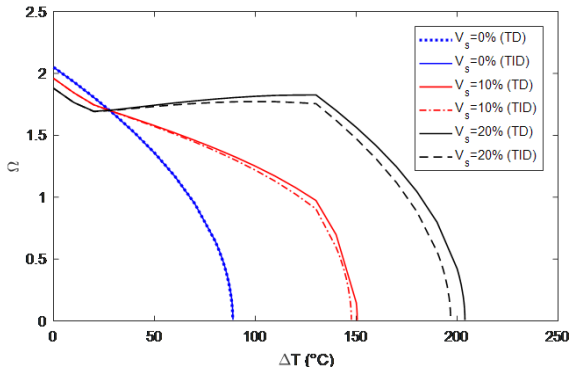

Fig. 4. Effect of temperature dependency of materials on vibrational behavior of $[30^o/-45^o/45^o/90^o]_s$ SMAHC skew plates with simply supported boundary conditions in pre-buckling region (a/b=1 , h/b=1/100 , e_0=0.02 , ψ=30°)

3- 3- Volume fraction of SMAs

Fig. 4 can also give some information about the role of the volume fraction of SMA wires in free vibrations of laminated composite skew plates. It is found that with the increase of temperature, the fundamental natural frequency of plates without SMA decreases continuously and it reaches to zero (buckling temperature), but the fundamental frequency parameter of structures with embedded SMAs first decreases, then increases to a maximum value and finally decreases to zero. It should be also noted that, as it can be observed from Fig. 4, more SMA wires lead to a higher fundamental frequency at temperatures above A_f. Unlike this region, when $T < A_f$ (ΔT < 30°), SMA volume fraction has a destructive role in the vibrational behavior of the structure. In other words, by increasing the embedded shape memory wires, the fundamental natural frequency of structure decreases when the temperature is below A_f. This is due to the fact that, in this region, plates with SMA wires have more density without producing tensile force to affect the stiffness of the structure. Therefore, embedding more SMA wires makes the structure heavy without any effects on the stiffness of structure and consequently results in a decrease in vibrational characteristics of the plate.

3- 4- Pre-strain of SMA fibers

The next parametric study is dedicated to show the influence of pre-strain of SMA wires on vibration characteristics of SMAHC skew plates. Fig. 5 confirms that variations of pre-strain do not have any significant influence. The figure also states that variations of pre-strain do not have any significant influence on free vibration of composite plates when $T < A_f$, but the role of pre-strain of SMA wires becomes more noticeable at higher temperatures. From numerical point of view, and as it is obvious from Fig. 5, by changing the value of ε_0 from 0.1% to 1% when ΔT=80°, the first natural frequency of composite skew plate improves up to 300% (from 0.4137 to 1.706).

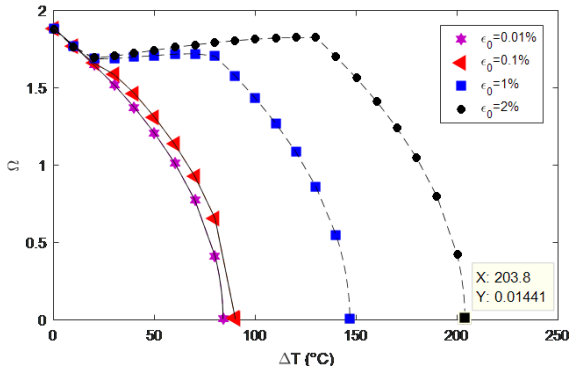

Fig. 5. Variations of fundamental frequency parameter of simply supported $[30^o/-45^o/45^o/90^o]_s$ SMAHC skew plates versus temperature for different values of SMA pre-strain (a/b=1 , h/b=1/100 , ψ=30°)

3- 5- Stacking sequence of layers

Now, variations of the fundamental natural frequency of simply supported SMAHC plates versus stacking sequence of layers is investigated at ΔT=100°. First, the changes of the first natural frequency of a square $[\theta/-\theta]_s$ composite plate are examined by focusing on Figs. 6(a-b) in which θ varies from -90° to 90°. As expected, the diagrams are symmetric with respect to θ=0° and state that the best lay-up for the plate in order to have the maximum fundamental frequency occurs in two cases of θ=-45° and θ=45°. Then, the natural frequency behavior of a $[\theta/-\theta]_s$ skew plates is depicted in Figs. 6(c-d). It is obvious that the skew angle (ψ=30°) causes the plate to have only one optimum solution for frequency maximization which is in the range of $-80^o \leq \theta \leq -60^o$ frequency maximization. Finally, the variations of the frequency of skew plates with a different lay-up, namely $[\theta/-45^o/45^o/90^o]_s$, versus θ are demonstrated in Figs. 6(e-f). By comparing these figures with Figs. 6(a-d) associated with $[\theta/-\theta]_s$ plates, it can be concluded that the stacking sequence

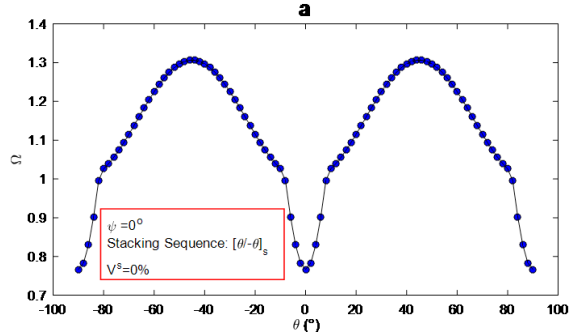

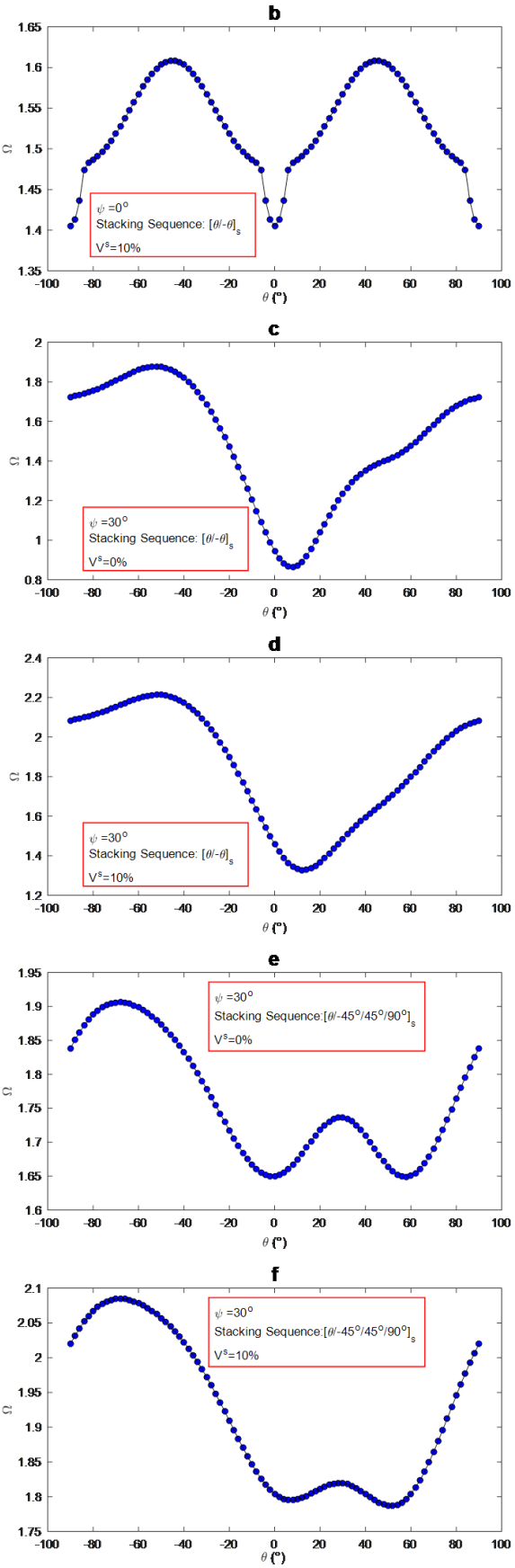

Fig. 6. Effect of stacking sequence of layers on fundamental frequency parameter of simply supported plates (*a*/*b*=1 , *h*/*b*=0.01 , e_0=0.02 , ΔT=100°C)

of layers can seriously change the variations trend of the natural frequency of SMAHC structures. It is clear that the new lay-up brings about a local maximum between 20° and 40°.

3- 6- Geometrical parameters and boundary conditions

Here, it is shown that how skew angle affects vibrational characteristics of SMAHC skew plates. From Fig. 7, the influence of skew angle on the fundamental natural frequency of the structure is illustrated for various SMA volume fractions when ΔT=100°C. It is found that, first, the frequency parameter increases until a local maximum point. Then, it decreases with the increase of skew angle up to a local minimum point. Finally, it increases with the increase of ψ. Fig. 7(a-d) show that embedding more SMA shifts the local maximum point to the left so that this point vanishes when V^s=25%. To clarify the reason for this phenomenon, one should simultaneously consider the effect of ψ on the stiffness of structure because of material properties and boundary conditions, thermal stresses resultants because of thermal environment, and recovery stress resultants induced by SMA fibers.

The effect of boundary conditions on the fundamental frequency of skew composite plates with respect to SMA volume fraction is tabulated in Table 5. The results reveal

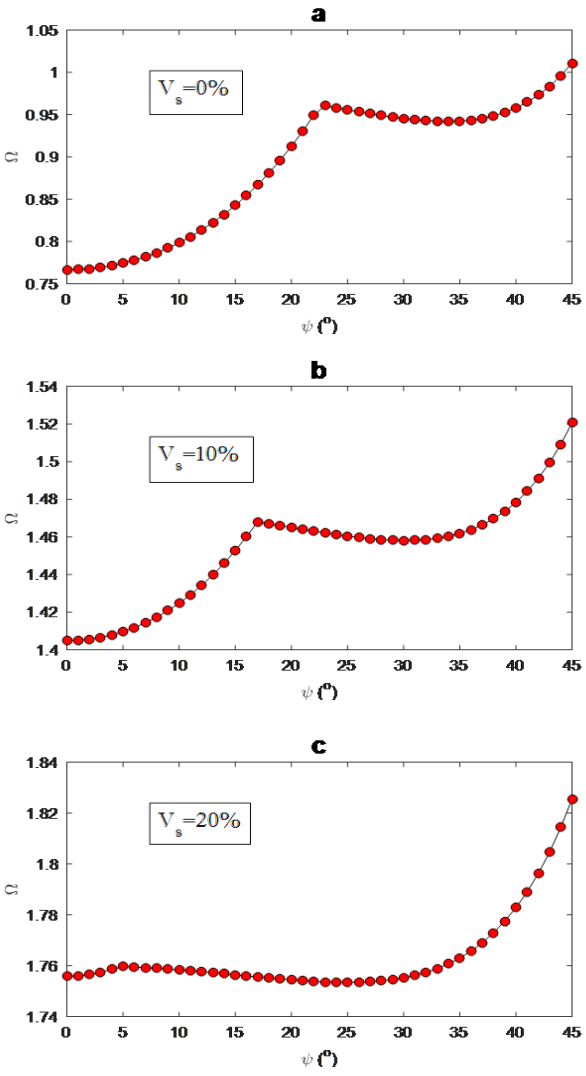

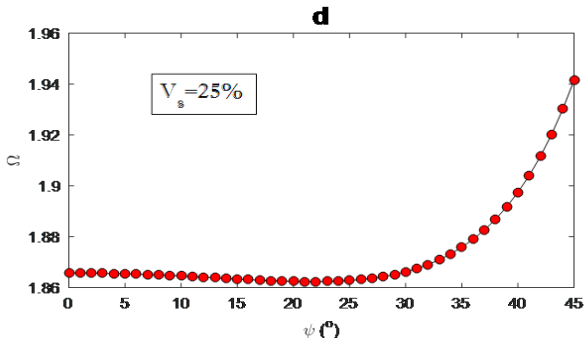

Fig. 7. Variation of fundamental frequency parameter of a simply supported SMAHC skew plate against skew angle and SMA volume fraction (a/b=1 , h/b=0.01 , e_0=2%)

Table 5. The effect of boundary conditions on the first four natural frequency parameters of [30°/-45°/45°/90°]$_s$ SMAHC skew plates (h/b=0.02 , ψ=30% , e_0=2% , ΔT=100°C)

Boundary conditions	V^s			
	0%	5%	10%	20%
SSSS	1.737	1.780	1.819	1.888
SSSC	2.012	2.045	2.076	2.131
SCSC	2.367	2.387	2.407	2.444
SCCC	2.682	2.694	2.706	2.729
CCCC	3.121	3.120	3.120	3.123

that SMA volume fraction can decrease the role of boundary conditions on vibrational behavior of composite structures. The results presented in Table 5 show that the fundamental frequency parameter of CCCC skew plates without SMA is about 80% higher than that of SSSS ones while this difference is about 65 % when the structure is embedded with 20% SMAs. The numerical comparison also specifies that the volume fraction of SMAs has more effect on the plate with simply supported boundaries. This is because plates with more clamped boundaries have a higher stiffness which is not affected by SMA wires as easily as the stiffness of simply supported ones.

4- Conclusion

This study presents free vibration analysis of SMAHC skew plates. The behavior of SMA wires was modeled by Brinson approach and the natural frequencies of the structure were obtained by employing GDQ method. The influences of SMA volume fraction, lamination scheme, pre-strain of SMA fibers, temperature, and dependency of material properties on the natural frequency response of SMAHC skew plates were examined. The numerical results represent that SMAs can seriously affect the vibrational behavior of composite structures.

References

[1] W. Li, Y. Li, Vibration and sound radiation of an asymmetric laminated plate in thermal environments, *Acta Mechanica Solida Sinica*, 28(1) (2015) 11-22.

[2] X. Li, K. Yu, J. Han, H. Song, R. Zhao, Buckling and vibro-acoustic response of the clamped composite laminated plate in thermal environment, *International Journal of Mechanical Sciences*, 119 (2016) 370-382.

[3] A.M. Zenkour, Thermal bending of layered composite plates resting on elastic foundations using four-unknown shear and normal deformations theory, *Composite Structures*, 122 (2015) 260-270.

[4] K. Marynowski, Free vibration analysis of an axially moving multiscale composite plate including thermal effect, *International Journal of Mechanical Sciences*, 120 (2017) 62-69.

[5] Y. Fan, H. Wang, Nonlinear bending and postbuckling analysis of matrix cracked hybrid laminated plates containing carbon nanotube reinforced composite layers in thermal environments, *Composites Part B: Engineering*, 86 (2016) 1-16.

[6] M.K. Singha, L. Ramachandra, J. Bandyopadhyay, Vibration behavior of thermally stressed composite skew plate, *Journal of sound and vibration*, 296(4) (2006) 1093-1102.

[7] R. Heuer, Equivalences in the analysis of thermally induced vibrations of sandwich structures, *Journal of Thermal Stresses*, 30(6) (2007) 605-621.

[8] S. Singh, A. Chakrabarti, Static, vibration and buckling analysis of skew composite and sandwich plates under thermo mechanical loading, *International Journal of Applied Mechanics and Engineering*, 18(3) (2013) 887-898.

[9] L.C. Brinson, One-dimensional constitutive behavior of shape memory alloys: thermomechanical derivation with non-constant material functions and redefined martensite internal variable, *Journal of intelligent material systems and structures*, 4(2) (1993) 229-242.

[10] R.-x. Zhang, Q.-Q. Ni, A. Masuda, T. Yamamura, M. Iwamoto, Vibration characteristics of laminated composite plates with embedded shape memory alloys, *Composite structures*, 74(4) (2006) 389-398.

[11] R. Yongsheng, S. Shuangshuang, Large amplitude flexural vibration of the orthotropic composite plate embedded with shape memory alloy fibers, Chinese *Journal of Aeronautics*, 20(5) (2007) 415-424.

[12] F. Forouzesh, A.A. Jafari, Radial vibration analysis of pseudoelastic shape memory alloy thin cylindrical shells by the differential quadrature method, *Thin-Walled Structures*, 93 (2015) 158-168.

[13] A. Parhi, B. Singh, Nonlinear free vibration analysis of shape memory alloy embedded laminated composite shell panel, *Mechanics of Advanced Materials and Structures*, 24(9) (2017) 713-724.

[14] M.B. Dehkordi, S. Khalili, E. Carrera, Non-linear transient dynamic analysis of sandwich plate with composite face-sheets embedded with shape memory alloy wires and flexible core-based on the mixed LW (layer-wise)/ESL (equivalent single layer) models, *Composites Part B: Engineering*, 87 (2016) 59-74.

[15] M. Samadpour, M. Sadighi, M. Shakeri, H. Zamani, Vibration analysis of thermally buckled SMA hybrid composite sandwich plate, *Composite Structures*, 119 (2015) 251-263.

[16] G.J. Turvey, I.H. Marshall, *Buckling and postbuckling of composite plates*, Springer Science & Business Media,

2012.

[17] C.W. Bert, M. Malik, Differential quadrature method in computational mechanics: a review, *Applied Mechanics Reviews*, 49 (1996) 1-28.

[18] P. Malekzadeh, G. Karami, Differential quadrature nonlinear analysis of skew composite plates based on FSDT, *Engineering Structures*, 28(9) (2006) 1307-1318.

[19] T. Kant, C. Babu, Thermal buckling analysis of skew fibre-reinforced composite and sandwich plates using shear deformable finite element models, *Composite Structures*, 49(1) (2000) 77-85.

[20] A. Vosoughi, P. Malekzadeh, M.R. Banan, M.R. Banan, Thermal postbuckling of laminated composite skew plates with temperature-dependent properties, *Thin-Walled Structures*, 49(7) (2011) 913-922.

[21] K. Malekzadeh, A. Mozafari, F.A. Ghasemi, Free vibration response of a multilayer smart hybrid composite plate with embedded SMA wires, *Latin American Journal of Solids and Structures*, 11(2) (2014) 279-298.

[22] H. Asadi, M. Eynbeygi, Q. Wang, Nonlinear thermal stability of geometrically imperfect shape memory alloy hybrid laminated composite plates, *Smart Materials and Structures*, 23(7) (2014) 075012.

Please cite this article using:

S. Kamarian and M. Shakeri, Natural Frequency Analysis of Composite Skew Plates with Embedded Shape Memory Alloys in Thermal Environment, *AUT J. Mech. Eng.*, 1(2) (2017) 179-190.

DOI: 10.22060/mej.2017.12655.5389